Summer Student Project Report

10 September 2021
salvati.flavio@cern.ch

Measuring K_s^0 and Λ abundances in QCD Instanton induced processes.

Flavio Salvati
Supervisors: Tancredi Carli, Matthias Schott

Abstract:

In this project we studied the abundances of strange K_s^0 and Λ particles in MC-Instanton and MC-EPOS samples. By comparing our results to ATLAS data, we assessed the suitability of these observables in the experimental detection of QCD Instanton induced processes at the LHC. We proceeded by selecting appropriate filters on tracks and V0 vertices that maximise the significance of the K_s^0 and Λ peaks, as well as reducing the false-positive rate and increasing the efficiency of detection. Having shown that both hadrons can be reconstructed with similar efficiencies in Instanton and EPOS samples, we studied their relative abundances in intervals of constant track number. Our analysis showed no measurable difference of K_s^0 and Λ production in QCD Instanton induced processes.

Contents

1 Introduction

Instantons are constant energy solutions to quantum mechanical equations of motion, associated with critical points of the action. These localised and inherently non-perturbative processes can be thought of as an ongoing rearrangement of the vacuum [5]. The simplest example of an Instanton solution can be found in the semi-classical approximation (SCA) for the path integral representation, leading to tunneling processes in imaginary time, an approach first carried out by Polyakov et al. [7] Several pertinent aspects of the SCA generalise to four-dimensional Euclidean Yang-Mills theory. The minima of the classical Yang-Mills action are determined by the topology of the gauge group and give rise to the periodic potential plotted in Fig. 1 as a function of the Chern-Simons (or winding number), $N_{\rm CS}$. In this framework, Instantons describe tunneling transitions in Minkowski spacetime between classically degenerate vacua, which only differ in their winding number by one unit, i.e. $\Delta N_{\rm CS} = 1$. There also exists a second category of classical solutions, known as Sphalerons, corresponding to transitions from one vacuum by a half-integer winding number on top of the energy barrier (also shown in Fig. 1).

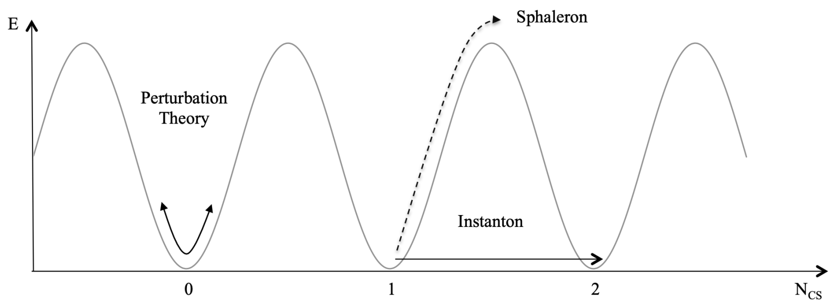

Figure 1: Energy density of the gauge field (y-axis) vs. winding number $N_{\rm CS}$ (x-axis) for Instanton and Sphaleron processes in a Yang-Mills vacuum. Diagram taken from [1].

Instantons and Sphalerons induce new physical phenomena without analogy in the quantum mechanical case, from B + L violation in the electroweak theory to chiral symmetry breaking [9, 10, 11] and the resolution of the axial U(1) problem [12] in the light-quark sector of QCD.

A QCD Instanton tunneling process between $\Delta N_{\rm CS} = 1$ vacua leads to the creation of a quark-antiquark pair of different chirality for N_f flavours, in association with a number n_g of additional gluons. We only consider the dominant contribution from gluon-gluon transition [1,2], which proceeds through the process:

$$g + g \to \sum_{f=1}^{N_f} (q_R^f + \overline{q}_L^f) + n_g g \,. \tag{1}$$

In the pseudo particle picture, this can be interpreted as a decay process of an Instanton pseudo particle with a mass m_I. For low Instanton masses, e.g. in the 20-80 GeV range, we expect therefore an isotropic decay into up to 5 quarks, 5 anti-quarks as well as 5-10 gluons. As a consequence, QCD Instanton-induced scattering processes produce soft bombs

– very high-multiplicity spherically symmetric distributions of relatively soft particles [7]. Experimentally, m_I can be approximated by the 4-vector sum of all charged particles with a certain minimal transverse momentum. For this reason, highly interesting is the distribution of K_s^0 and Λ, as more heavy quarks in the final state of the Instanton decays are expected, which typically hadronize to longer lived mesons and hadrons.

2 Improving the significance of the peak

Particles like K_s^0 and Λ travel a short but recognisable distance from their birth place (primary vertex) and then decay into children particles at the secondary vertex. From the many packages/finders that ATLAS has developed for secondary vertexing, we will use one which was specifically designed for K_s^0 and Λ reconstruction, the InDetV0FinderTool. This finder runs over all pairs of opposite-sign tracks and performs an unconstrained two-particle vertex fit to a V0 vertex. V0 candidates with a χ^2 probability $> 1 \cdot 10^4$ are recorded during event reconstruction, forming a set of pre-selected V0 vertices. These two-track vertices are fitted with each of the $K_s^0 \to \pi^+\pi^-$, $\Lambda \to p\,\pi^-$ and $\overline{\Lambda} \to p^-\,\pi^+$ particle hypotheses for the positive and negative tracks. The resultant fit parameters for these three cases, along with element links to the two tracks, are decorated onto the vertex and recorded in the AOD during reconstruction. From this, we can immediately plot the invariant mass of pairs of tracks which are associated to a K_s^0 or Λ in the V0 reconstruction (see Fig. 2).

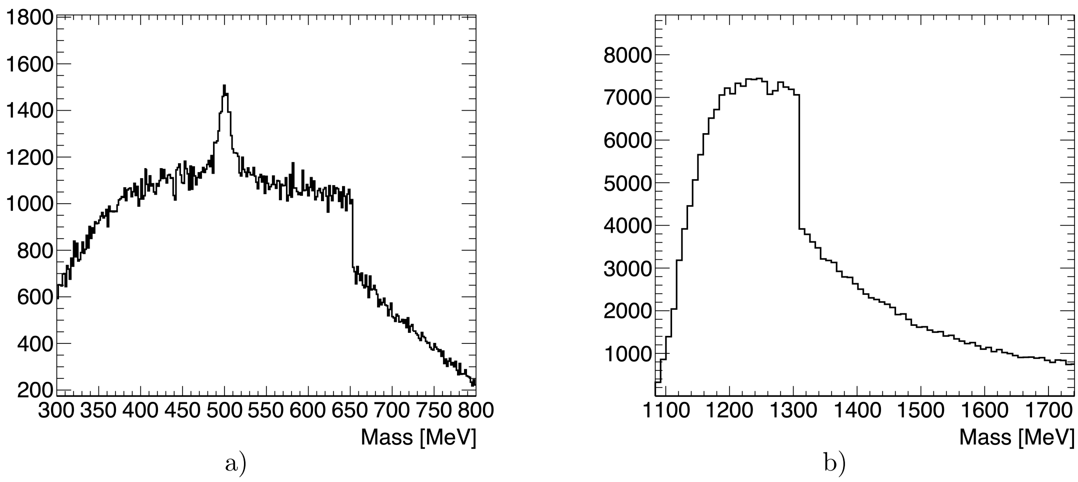

Figure 2: a) K_s^0 and b) Λ peaks as obtained directly from the InDetV0FinderTool over 8500 MC-EPOS events. The K_s^0 peak at 497.611 MeV clearly stands out of the background, while the Λ peak at 1115.683 MeV is not visible.

No lower track P_t cut or track quality requirements are imposed on the input tracks considered by the tool. This motivates our search for preliminary cuts on tracks and additional cuts on V0 vertices, with the aim of increasing the significance of the K_s^0 and Λ peaks.

2.1 Track Selection

The following filters were applied on the tracks:

1. Track not fitted to a Primary Vertex (PV)
2. 1.0 mm $< d_0 <$ 25 mm
3. $z_0 <$ 50 mm
4. SCT Hits > 3
5. Pixel Hits > 2
6. Next to Innermost Pixel Hits > 0

The transverse impact parameter d_0 is conventionally defined as the shortest distance between a track and the beam line in the transverse plane, while the longitudinal impact parameter z_0 is the distance along the beam line from the PV to the point on the track used to evaluate d_0 (see Fig. 3).

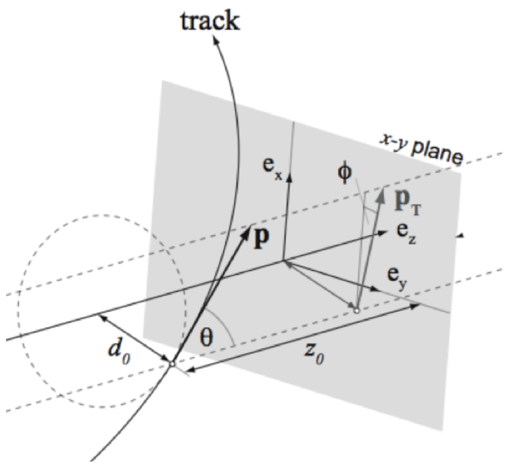

Figure 3: Transverse and longitudinal impact parameters d_0 and z_0. The centre of the coordinate system is the Primary Vertex.

To correct for the position of the beam line and the PV, we redefined d_0 and z_0 as follows:

$$d_0 \rightarrow \sqrt{(\mathrm{PV}_x - \mathrm{Beam}_x)^2 + (\mathrm{PV}_y - \mathrm{Beam}_y)^2} - d_0\,, \tag{2}$$

$$z_0 \rightarrow \mathrm{Beam}_z - \mathrm{PV}_z + z_0\,, \tag{3}$$

where $\mathrm{Beam}_{x,y,z}$ and $\mathrm{PV}_{x,y,z}$ are the Cartesian coordinates of the beam line and the Primary Vertex, respectively. Since the PV lies on the beam line, the term under the square root in Eq. 2 represents a very small correction, typically on the order of $0.01 - 0.1$ mm. The correction on z_0 is more significant, being on the order of $10 - 100$ mm. As a sanity check, the distributions of d_0 and z_0 for particle tracks in one event are plotted in Fig. 4. After the correction is applied, the distributions become symmetric about $d_0 = z_0 = 0$.

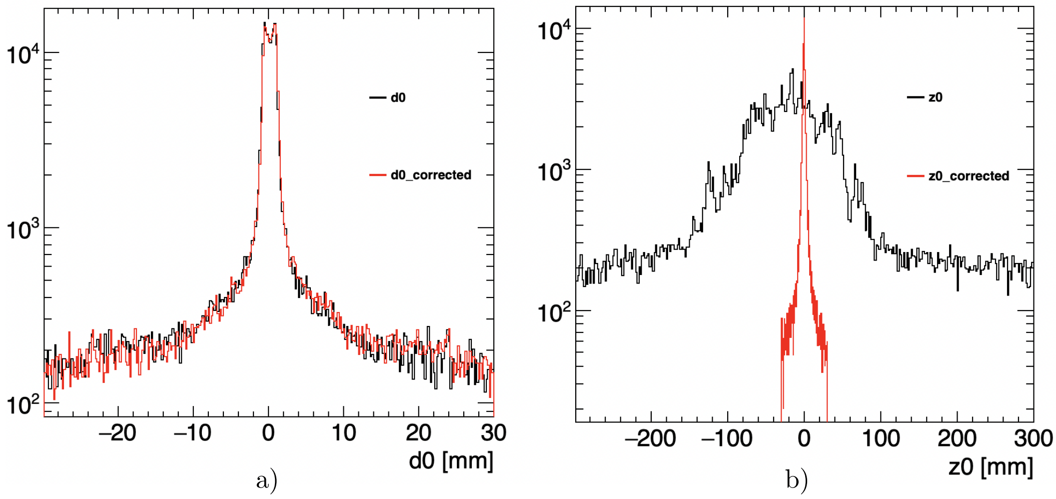

Figure 4: a) d0 b) z0 with and without beamline correction.

We will perform our optimisation procedure on the K_s^0 only, as it is more straightforward to see how this affects the significance of the peak. We will return to the Λ analysis once all our track filters have been optimised.

As a starting point, we apply filter 1 (!PriVtx), as we expect V0 tracks to be a worse fit to the PV. As shown in Fig. 5 a), this results in a substantial improvement in significance. b) and c) show the K_s^0 peak when a low and high d_0 filter is applied. The best significance is obtained choosing $d_0 > 1\,\mathrm{mm}$ and $d_0 < 25\,\mathrm{mm}$. In d) and e) we test a similar filter on the z_0, but only observe an increase in significance for $z_0 < 50\,\mathrm{mm}$. In e), f) and g) the track hits are studied, and we conclude that the best filters are SCTHits> 3, PixHits> 2 and NextToInnPixHits> 0.

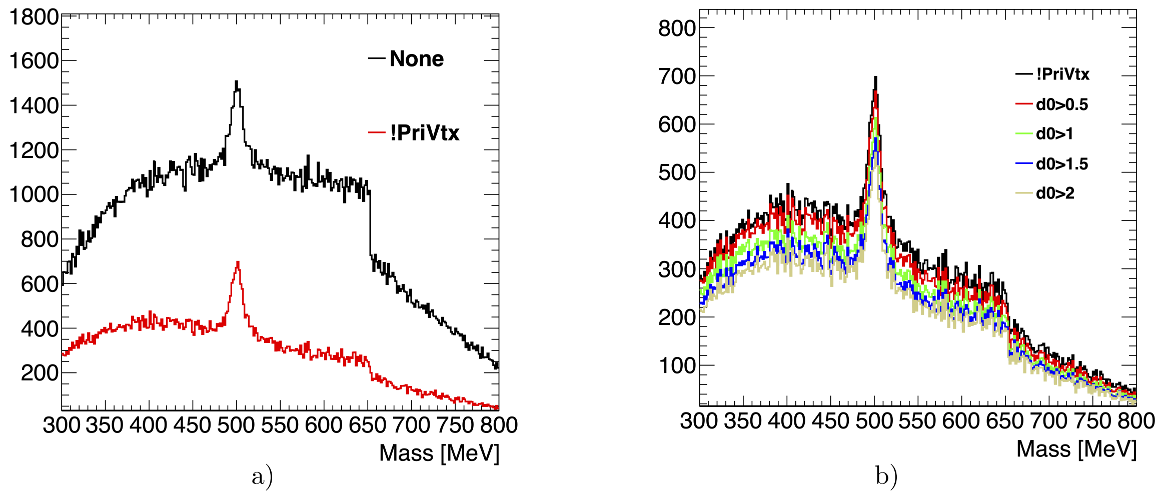

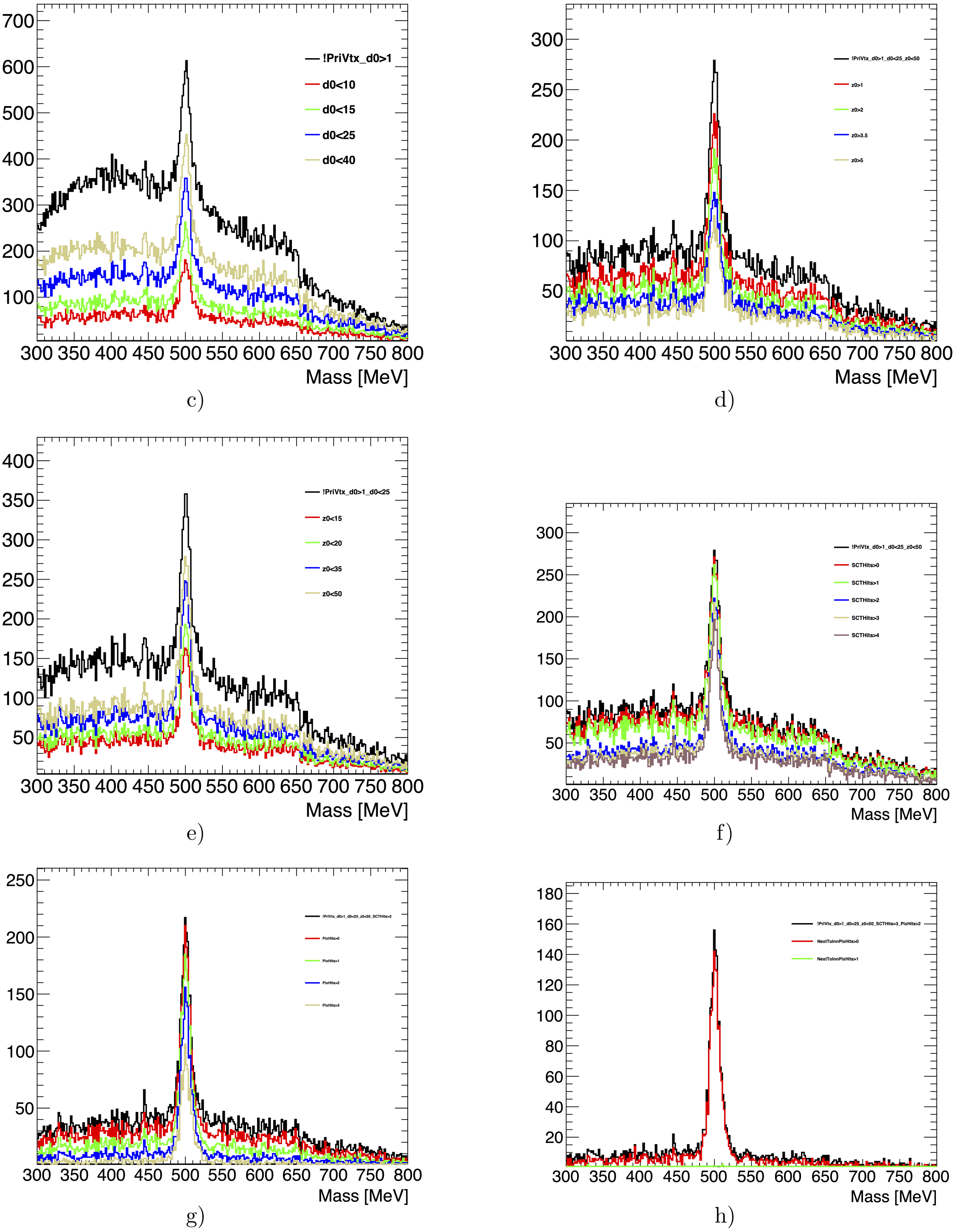

Figure 5: Vetoes giving higher signal/background ratio: a) !PriVtx, b) $d_0 > 1.5$ mm , c) $d_0 < 25$ mm, d) $z_0 < 50$ mm, e) no low d0 veto, f) SCTHits > 3, g) PixHits> 2, h)NextToInnPixHits > 0. In each case, the best cut is added to the base filter and used in the next selection.

2.2 V0 Selection

Selection cuts and vetoes are applied to the pre-selected V0 vertices to identify K_s^0 and Λ candidates. The cuts are inspired by the ATLAS 7 TeV paper [3] and by Tim Martin's notes [4]. The $\chi^2 < 7$ cut is common to both the K_s^0 and Λ.
The subsequent requirements on a V0 to be classified as K_s^0 are:

- $P_t > 400\,\mathrm{MeV}$
- $\cos\theta > 0.999$, i.e. $\theta < 2.6°$
- $4\,\mathrm{mm} < R_{xy} < 300\,\mathrm{mm}$

The subsequent requirements on a V0 to be classified as Λ are:

- $P_t > 700\,\mathrm{MeV}$
- $\cos\theta > 0.9998$, i.e. $\theta < 1.1°$
- $15\,\mathrm{mm} < R_{xy} < 300\,\mathrm{mm}$

where P_t is the reconstructed transverse momentum of the candidate K_s^0 or Λ, R_{xy} its decay radius in the transverse plane, and θ is the three dimensional opening angle between the vector connecting the PV to the V0, and the V0's momentum vector w.r.t the PV, i.e.:

$$\cos\theta = \frac{\vec{r}\cdot\vec{\mathrm{V0}}_p}{|r||\mathrm{V0}_p|} \quad \text{with} \quad \vec{r} = \vec{\mathrm{V0}}_r - \vec{\mathrm{PV}}_r \tag{4}$$

2.3 Results

Applying both the track and V0 selections to the MC-EPOS and ATLAS data samples, we observe a symmetric peak around the known mass values [6] of $497.611 \pm 0.013\,\mathrm{MeV}$ for K_s^0 and $1115.683 \pm 0.006\,\mathrm{MeV}$ for Λ (Fig. 6). The V0 filter further decreases the background by a factor of 10, giving a signal to background ratio of more than 100 for K_s^0, and around 30 for the Λ.

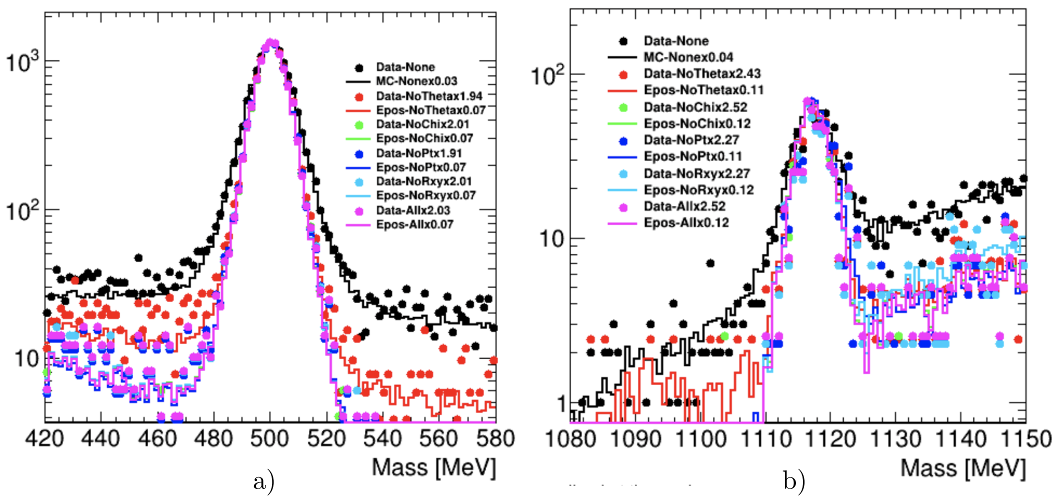

Figure 6: a) K_s^0 b) Λ mass peaks with track filters only (None), track and V0 filters (All), and All - one V0 filter at a time (All-Theta, All-Rxy, All-Pt, All-chi2). Data and MC-EPOS show excellent agreement.

3 Maximising efficiency and significance

3.1 Truth Selection

The strange particle selection requires the following. An initial pre-selection for K_s^0:

- PID parent = 310 (K_s^0)
- PID children = $\pm 211(\pi^{\pm})$ and $\mp 211(\pi^{\mp})$
- $P_t > 400\,\text{MeV}$

And Λ:

- PID parent = 3122 (Λ)
- PID children = $\pm 2212(\text{p}^{\pm})$ and $\mp 211(\pi^{\mp})$
- $P_t > 700\,\text{MeV}$

where P_t is the transverse momentum of the parent. We also require the tracks associated to a truth particle to have a truth match probability of $P_{\text{match}} > 0.5$, defined as follows:

$$P_{\text{match}} = \frac{10 \cdot N_{\text{Pixel}}^{\text{common}} + 5 \cdot N_{\text{SCT}}^{\text{common}} + 1 \cdot N_{\text{TRT}}^{\text{common}}}{10 \cdot N_{\text{Track}}^{\text{common}} + 5 \cdot N_{\text{Track}}^{\text{common}} + 1 \cdot N_{\text{Track}}^{\text{common}}},$$

matching truth particles to tracks via common hits.
For example, the truth calculation in one event proceeds as follows:

1. Start from the list of V0 pairs, and select only those pairs whose tracks are associated to truth particles and truth parents passing the above defined selections.
2. Create a list of selected V0 pairs containing pointers to the truth particles of the corresponding tracks.
3. Select only unique pairs from the above list, since one particle can be matched to one or more tracks. The length of this list gives the number of truth parents n_{truth}.

Next, we find the truth-reconstructed number of V0 vertices as follows:

4. Using the filters defined in Sections 2.1 and 2.2, obtain a list of candidate V0 pairs. By requiring the V0 pairs to have an invariant mass of 20 MeV from the peak, find the list of reconstructed V0 pairs.
5. The truth-reconstructed V0 list is the intersection of the truth and reconstructed V0 lists.
6. Repeat steps 2 and 3 on the truth-reconstructed V0 list to find $n_{\text{truth}}^{\text{reco}}$.

We can then compute the efficiency as:

$$\text{eff} = \frac{n_{\text{truth}}^{\text{reco}}}{n_{\text{th}}}. \tag{5}$$

3.2 Increasing the efficiency

The resulting efficiency when all filters discussed in Sections 2.1 and 2.2 are applied is only 18 % for K_s^0 and 8 % for Λ. We now study which track filters lead to the best trade-off between efficiency and significance of the peak, while leaving the V0 filters unaltered. Looking at every possible combination of filters would be unfeasible, therefore we proceed by first applying each filter individually, and selecting only those that lead to a better compromise between the two parameters defined above. We then examine all combinations of selected filters and choose the best overall. Fig. 7 shows individual filters applied to an EPOS file. There are only three filters which lead to an overall improvement, i.e. !PriVtx, SCTHits>3 and $d_0 > 1$ mm. Since the filter !PriVtx shows the best overall contribution, we use this as our base filter when examining all combinations of the other two selected filters (see Fig. 8). The best track filter is then found to be the intersection of !PriVtx and SCTHits>3. Repeating the same analysis for the Instanton sample (Figs. 9 and 10), we see that the best filter in this case is the intersection of !PriVtx, SCTHits>3 and $d_0 > 1$. We decide to take a common filter in the two cases, therefore we choose:

- !PriVtx
- SCTHits > 3

The resulting efficiencies on the MC-EPOS and MC-Instanton samples are 41.4% and 44.6%, while the corresponding signal to background ratios are 19.7 and 11.3, respectively.

Track Filter	# Events	# Truth	# Truth & Rec	Efficiency [%]	Sig/Bkg
No Filter	8500	4725	2214	46.9	10.8
SCTHits>3	8500	4725	2011	42.5 -9%	13.5 +25%
PixHits>2	8500	4725	1832	33.2 -30%	13.7 +27%
NextToInnPixHits>0	8500	4725	1429	30.2 -35%	13.1 +21%
!PriVtx	8500	4725	2149	45.5 -3%	15.6 +44%
d0<25	8500	4725	1045	39.7 -15%	11.0 +2%
d0>1	8500	4725	1860	42.1 -10%	17.1 +58%
z0<50	8500	4725	1237	41.1 -12%	13.0 +20%

Figure 7: EPOS efficiency for every track filter taken individually.

Track Filter	# Events	# Truth	# Truth & Rec	Efficiency [%]	Sig/Bkg
!PriVtx	8500	4725	2214	45.5	15.6
+SCTHits>3	8500	4725	1956	41.4 -9%	19.7 +26%
+d0>1	8500	4725	1845	39.0 -14%	18.1 +16%
+SCTHits>3 +d0>1	8500	4725	1687	35.7 -21%	19.9 +27%

Figure 8: EPOS efficiency for combinations of the best two track filters.

Track Filter	# Events	# Th	# Th & Rec	Efficiency	Sig/Bkg
No Filter	8500	6380	2214	49.7	4.5
SCTHits>3	8500	6380	2932	46.0 -7%	6.2 +38%
PixHits>2	8500	6380	2558	38.1 -21%	5.6 +17%
NextToInnPixHits>0	8500	6380	1901	29.8 -40%	5.5 +22%
!PriVtx	8500	6380	3116	48.8 -2%	7.2 +60%
d0<25	8500	6380	1253	28.6 -43%	4.2 -7%
d0>1	8500	6380	2767	44.2 -11%	10.4 +130%
z0<50	8500	6380	1486	36.1 -28%	5.4 +24%

Figure 9: Instanton efficiency for every track filter taken individually.

Rec. Filter	# Events	# Th	# Th & Rec	Efficiency	Sig/Bkg
!PriVtx	8500	6380	3116	48.8	7.2
+SCTHits>3	8500	6380	2845	44.6 -9%	11.3 +57%
+d0>1	8500	6380	2718	42.6 -13%	13.2 +83%
+SCTHits>3 +d0>1	8500	6380	2539	39.8 -18%	15.8 +120%

Figure 10: Instanton efficiency for combinations of the best two track filters.

4 Comparing abundances of K_s^0 and Λ

In order to compare the number of K_s^0 and Λ in MC-Instanton, MC-EPOS and ATLAS data, we need all of them to be on an equal footing. Instanton induced processes typically have a larger number of tracks and a higher total invariant mass, therefore two possibilities come to mind: plot the number of reconstructed K_s^0 and Λ per event, in a given interval of track number or invariant mass per event. We choose the first route, selecting track numbers between 10-110, in intervals of 20 (Figs. 11 and 12, a-e).

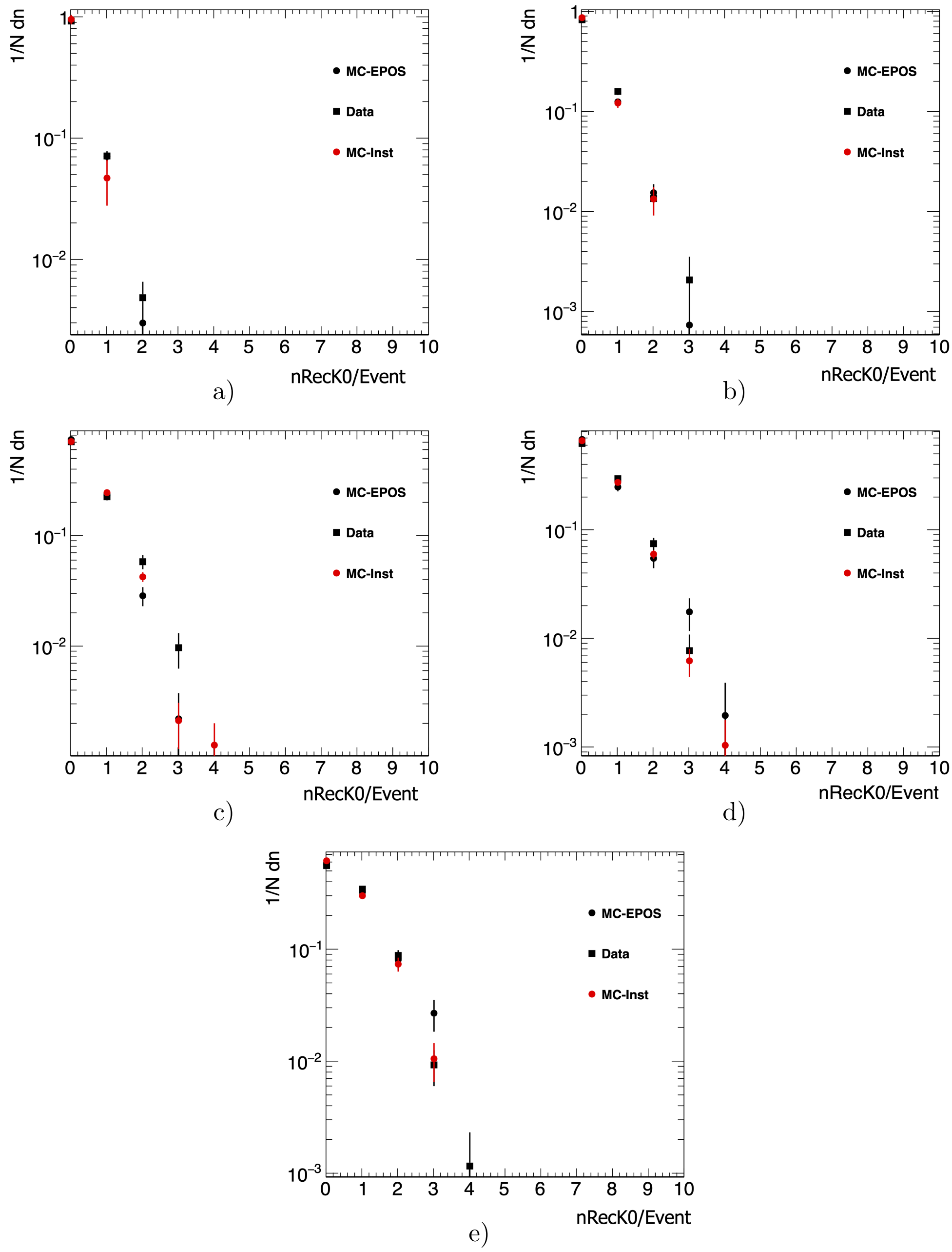

Figure 11: Number of reconstructed K_s^0 per event with track numbers between a) 10-30, b) 30-50, c) 50-70, d) 70-90, e) 90-110. Analysis is performed on MC-EPOS, ATLAS Data and MC-Instanton.

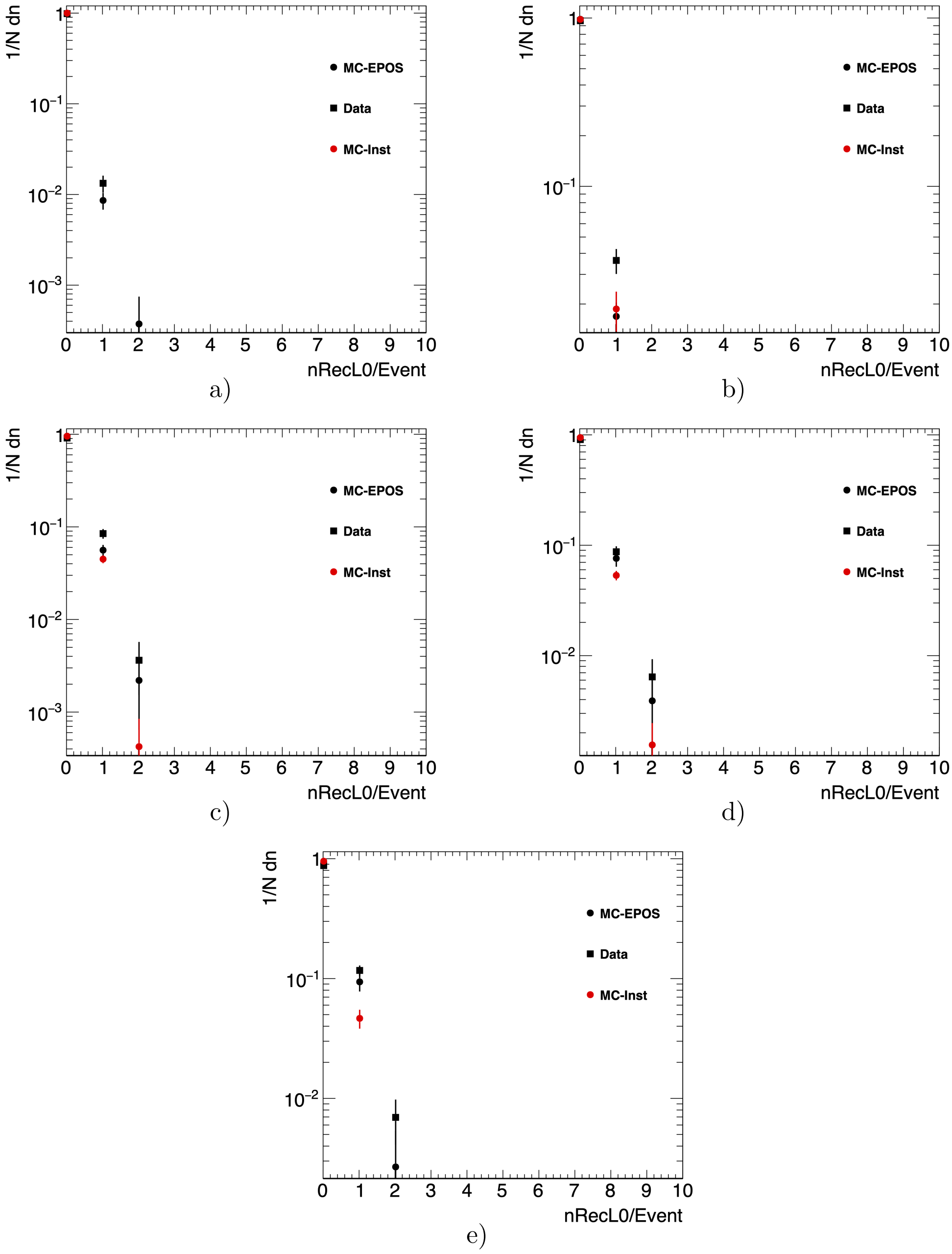

Figure 12: Number of reconstructed Λ per event with track numbers between a) 10-30, b) 30-50, c) 50-70, d) 70-90, e) 90-110. Analysis is performed on MC-EPOS, ATLAS Data and MC-Instanton.

5 Conclusion

In this report we have optimised the choice of track and V0 filters to reconstruct K_s^0 and Λ particles in MC-EPOS, MC-Instanton and ATLAS data, preserving the best significance, while maximising the efficiency of detection. In Section 3.2 we concluded that the best overall track filters are !PriVtx, SCTHits> 3, which together with the V0 filters in Section 2.2, lead to efficiencies of 41.4% and 44.6% on MC-EPOS and MC-Instanton samples, with corresponding signal to background ratios of 19.7 and 11.3, respectively.
Having found comparable efficiencies of detection, we compared the abundances of K_s^0 and Λ in QCD Instanton induced events and background. Since Instanton events typically have a larger number of tracks and a higher total invariant mass, we studied the number of reconstructed K_s^0 and Λ per event, in intervals of constant track numbers. Our analysis showed no measurable difference of K_s^0 and Λ production in MC-EPOS, MC-Instanton and ATLAS data.

Acknowledgements

I would like to thank my supervisors Tancredi Carli and Matthias Schott for the interesting research project and daily discussions over my 13-week internship. I am grateful to Tancredi for showing me around CERN for my very first time, even though the project this summer was entirely online due to Covid-19. I would also like to thank Ynyr Harris and all the other members of the Instanton group for providing me with all the tools and data I needed during my project.

References

[1] S. Amoroso, D. Kar, M Schott, How to discover QCD Instantons at the LHC, The European Physical Journal C volume 81, Article number: 624 (2021).

[2] Valentin V. Khoze, Frank Krauss, and Matthias Schott. Large Effects from Small QCD Instantons: Making Soft Bombs at Hadron Colliders. JHEP, 04:201, 2020.

[3] G. Aad et al., K_s^0 and Λ production in pp interactions at $\sqrt{s} = 0.9$ and 7 TeV measured with the ATLAS detector at the LHC, Phys. Rev. D85 (2012) 012001, arXiv: 1111.1297.

[4] T. Martin, Strange K_s^0 and Λ particle spectra at ATLAS as probes of the Underlying Event in pp interactions at $\sqrt{s} = 13$ TeV.

[5] T. Martin, Strange K_s^0 and Λ particle spectra at ATLAS as probes of the Underlying Event in pp interactions at $\sqrt{s} = 13$ TeV.

[6] C. Patrignani et al., Review of Particle Physics, Chin. Phys. C40 (2016) 100001.

[7] A. Polyakov, Nucl. Phys. B120, 429 (1977); see also E. Gildener and A. Patrascioiu, Phys. Rev. D 16, 423 (1977); J.F. Willemsen, Phys. Rev. D 20, 3292 (1979).

[8] Roni Harnik and Tommer Wizansky. Signals of New Physics in the Underlying Event. Phys. Rev. D, 80:075015, 2009.

[9] Gerard 't Hooft. Computation of the Quantum Effects Due to a Four-Dimensional Pseudoparticle. Phys. Rev., D14:3432–3450, 1976. [Erratum: Phys. Rev.D18,2199(1978)]

[10] Gerard 't Hooft. Symmetry Breaking Through Bell-Jackiw Anomalies. Phys. Rev. Lett., 37:8–11, 1976.

[11] Dmitri Diakonov and V. Yu. Petrov. A Theory of Light Quarks in the Instanton Vacuum. Nucl. Phys., B272:457–489, 1986.

[12] Gerard 't Hooft. How Instantons Solve the U(1) Problem. Phys. Rept., 142:357–387, 1986.